

# Self-referenced spectroscopy using plasmon waveguide resonance biosensor

Farshid Bahrami,<sup>1,\*</sup> Mathieu Maisonneuve,<sup>2</sup> Michel Meunier,<sup>2</sup> J. Stewart Aitchison,<sup>1</sup> and Mo Mojahedi<sup>1</sup>

<sup>1</sup>Department of Electrical and Computer Engineering, University of Toronto, Ontario, M5S 3G4, Canada

<sup>2</sup>Department of Engineering Physics, Ecole Polytechnique de Montreal, Montreal, H3C 3A7, Canada

\*farshid.bahrami@mail.utoronto.ca

**Abstract:** A plasmon waveguide resonance (PWR) sensor is designed, fabricated, and tested for self-referenced biosensing. The PWR sensor is able to support two different polarizations, TM and TE. The TM polarization has a large sensitivity to variations in the background refractive index while the TE polarization is more sensitive to the surface properties. The ability of the PWR sensor to simultaneously operate in both TM and TE modes is used to decouple the background index variations (bulk effects) from the changes in adlayer thickness (surface effects) via multimode spectroscopy. To benchmark the performance of the PWR, a conventional surface plasmon resonance (SPR) sensor is fabricated and tested under the same conditions.

©2014 Optical Society of America

OCIS codes: (280.4788) Optical sensing and sensors; (250.5403) Plasmonics.

## References and links

1. J. Homola, S. S. Yee, and G. Gauglitz, "Surface plasmon resonance sensors: review," *Sens. Actuators B Chem.* **54**(1-2), 3–15 (1999).
2. G. G. Nenninger, J. B. Clendenning, C. E. Furlong, and S. S. Yee, "Reference-compensated biosensing using a dual-channel surface plasmon resonance sensor system based on a planar lightpipe configuration," *Sens. Actuators B Chem.* **51**(1-3), 38–45 (1998).
3. S. Nizamov and V. M. Mirsky, "Self-referencing SPR-biosensors based on penetration difference of evanescent waves," *Biosens. Bioelectron.* **28**(1), 263–269 (2011).
4. J. Guo, P. D. Keathley, and J. T. Hastings, "Dual-mode surface-plasmon-resonance sensors using angular interrogation," *Opt. Lett.* **33**(5), 512–514 (2008).
5. M. Maisonneuve, I. H. Song, S. Patskovsky, and M. Meunier, "Polarimetric total internal reflection biosensing," *Opt. Express* **19**(8), 7410–7416 (2011).
6. F. Bahrami, M. Maisonneuve, M. Meunier, J. S. Aitchison, and M. Mojahedi, "An improved refractive index sensor based on genetic optimization of plasmon waveguide resonance," *Opt. Express* **21**(18), 20863–20872 (2013).
7. D. P. Edward, *Handbook of optical constants of solids* (Academic Press, 1997).
8. F. Bahrami, M. Z. Alam, J. S. Aitchison, and M. Mojahedi, "Dual Polarization Measurements in the Hybrid Plasmonic Biosensors," *Plasmonics* **8**(2), 465–473 (2013).
9. S. Ltd, <http://www.ssens.nl/>.
10. M. Inc, <http://www.proteinslides.com/>.
11. M. Piliarik and J. Homola, "Surface plasmon resonance (SPR) sensors: Approaching their limits?" *Opt. Express* **17**(19), 16505–16517 (2009).
12. S. Janz, A. Densmore, D. X. Xu, W. Sinclair, J. H. Schmid, R. Ma, M. Vachon, J. Lapointe, A. Del age, E. Post, Y. Li, T. Mischki, G. Lopinski, P. Cheben, and B. Lamontagne, "Silicon photonic wire evanescent field sensors: From sensor to biochip array," 6th IEEE International Conference on Group IV Photonics, (2009).
13. J. Spinke, M. Liley, F. J. Schmitt, H. J. Guder, L. Angermaier, and W. Knoll, "Molecular recognition at self-assembled monolayers: Optimization of surface functionalization," *J. Chem. Phys.* **99**(9), 7012–7019 (1993).

## 1. Introduction

Over the past decades several optical methods have been used to investigate thin biomolecular films. Surface plasmon resonance (SPR) spectroscopy is one such a method which is commonly used for this purpose [1]. SPR sensors have high sensitivity due to their large

field intensity at the metal/dielectric interface. However, due to the field penetration beyond the interface, any variations within the penetration depth can also change the SPR propagation constant which results in a change in the output signal used for detection. Parameters which can alter the SPR propagation constant belong to two general categories: 1) *surface effects* which include thickness and refractive index of a biomolecular film also called adlayer. 2) *Bulk effects* which contain variations in the refractive index of the bulk solution flowing above the adlayer (these variations can be due to changes in the buffer concentration and/or temperature). Unfortunately, conventional SPR sensors cannot distinguish between the aforementioned surface and bulk effects so they need a reference channel to compensate for the bulk index variations [2]. To eliminate the need for a reference channel and therefore reduce the complexity, “self-referenced” sensors are developed which utilize two modes on the same channel to compensate for the bulk index change. Self-reference sensors commonly utilize dual-wavelength spectroscopy [3], dual-mode spectroscopy [4], and/or polarimetric total internal reflection [5].

In this paper a new approach based on a plasmon waveguide resonance (PWR) sensor is reported for self-referenced measurement. The PWR sensor, a thin metallic layer loaded with a dielectric layer [Fig. 1(a)]. The main feature of the PWR sensor is its capability to guide two different polarizations (transverse electric, TE, and transverse magnetic, TM) instead of the single TM polarization in the case of conventional SPR sensor. We have recently reported that the performance of the PWR sensor can exceed that of the SPR sensor for refractive index sensing applications [6]. Here, we report a self-referenced PWR sensor which is used to decouple the variations in bulk index and thin film thickness by utilizing both TM and TE polarizations.

## 2. Principle of operation

Angular spectroscopy using the Kretschmann configuration was chosen to monitor the propagation constant of the PWR modes by measuring the reflected light intensity [Fig. 1(a)]. Figure 1(b) illustrates the spatial distribution of the power density (Poynting vector) for both TE and TM modes of the optimized PWR sensor. The large penetration depth of the TM mode [black line in Fig. 1(b)] makes it suitable for probing the variations in the bulk refractive index. On the other hand, the small penetration depth of the TE mode [red line in Fig. 1(b)] makes it highly sensitive to the refractive index variations at the dielectric/water interface. Figure 1(c) shows the reflectance spectrum calculated using a transfer matrix method for both polarizations. For our calculations we have used the material optical properties listed in Palik [7].

Change in the bulk refractive index and/or surface binding result in different shifts for the TM and TE resonance angles ( $\Delta\theta_{TM}$  and  $\Delta\theta_{TE}$ , respectively). Assuming a linear relation between the resonance angles shift and the surface and bulk effects, the shifts for both polarizations are given by [8]:

$$\Delta\theta_{TM} = SF_{TM}^{bulk} \Delta n_B + SF_{TM}^{surf} \Delta d_a, \quad (1)$$

$$\Delta\theta_{TE} = SF_{TE}^{bulk} \Delta n_B + SF_{TE}^{surf} \Delta d_a, \quad (2)$$

where,  $SF_{TM}^{bulk}$  and  $SF_{TE}^{bulk}$  are the bulk sensitivity factors, in degree/refractive index unit (RIU), for the TM and TE polarizations, respectively. Similarly, the  $SF_{TM}^{surf}$  and  $SF_{TE}^{surf}$  are surface sensitivity factors in degree/nanometer for TM and TE polarizations, respectively. Lastly,  $\Delta n_B$

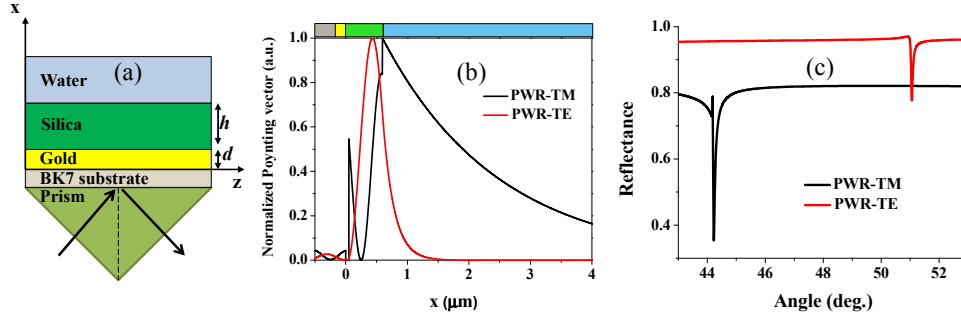


Fig. 1. (a) Schematic diagram of the PWR sensor. (b) z-component of the Poynting vector for both TM and TE polarizations in the optimized PWR sensor with  $h = 545\text{nm}$  and  $d = 49\text{nm}$  at the wavelength of  $780\text{nm}$ . (c) Reflectance spectrum for the optimized PWR-TM, PWR-TE in black and red lines, respectively.

and  $\Delta d_a$  are the changes in bulk refractive index and adlayer thickness, respectively. By measuring  $\Delta\theta_{TM}$  and  $\Delta\theta_{TE}$  and assuming that the sensitivity factors are known (for example, calculated from simulation or measured during calibration steps), Eqs. (1) and (2) can be used to calculate the quantities of interest (i.e.  $\Delta n_B$  and  $\Delta d_a$ ) according to:

$$\Delta n_B = \frac{SF_{TM}^{bulk} \times \Delta\theta_{TE} - SF_{TE}^{bulk} \times \Delta\theta_{TM}}{SF_{TM}^{bulk} \times SF_{TE}^{surf} - SF_{TM}^{surf} \times SF_{TE}^{bulk}}, \quad (3)$$

$$\Delta d_a = \frac{SF_{TE}^{surf} \times \Delta\theta_{TM} - SF_{TM}^{surf} \times \Delta\theta_{TE}}{SF_{TM}^{bulk} \times SF_{TE}^{surf} - SF_{TM}^{surf} \times SF_{TE}^{bulk}}, \quad (4)$$

### 3. Optimization

One of our goals was to compare the performance of our PWR sensor (with both TM and TE polarizations) with that of a conventional SPR sensor (only TM mode is allowed) fabricated and tested under the same conditions. In order to optimize the performances of our PWR and SPR sensors we used the genetic algorithm to determine the wavelengths of operation and layer thicknesses which maximizes the Figure of Merit (FoM) associated with each sensor. Our FoM is based on the Combined Sensitivity Factor (CSF) which is the product of the sensor's sensitivity [also called the Sensitivity Factor (SF)], and the ratio of the reflection spectrum depth ( $R_{max}-R_{min}$ ) and spectral line-width ( $FWHM$ ) given by [8]:

$$CSF_{bulk} = SF_{bulk} \times SM = \frac{\partial\theta_{res}}{\partial n_B} \times \frac{R_{max} - R_{min}}{FWHM}, \quad (5)$$

$$CSF_{surf} = SF_{surf} \times SM = \frac{\partial\theta_{res}}{\partial d_a} \times \frac{R_{max} - R_{min}}{FWHM}. \quad (6)$$

In Eqs. (5) and (6), the  $CSF_{bulk}$  and  $CSF_{surf}$  are the  $CSF$  defined for bulk and surface sensing applications, respectively. Since in the case of PWR sensor the TM mode is used to monitor the bulk effects (due to its large penetration into the fluid) and the TE mode is used to monitor the surface effects (due to its small penetration into the fluid) the appropriate FoM for the PWR sensor is:

$$FoM_{PWR} = CSF_{bulk}^{TM} \times CSF_{surf}^{TE}. \quad (7)$$

On the other hand, the FoM in the case of the SPR sensor (only TM mode) is defined for surface sensing applications according to:  $FoM_{SPR} = CSF_{surf}^{TM}$ . Lastly, it is important to note

that as discussed in [8], the CSF (and hence the FoM) is inversely proportional to the Limit of Detection (LoD).

Table 1 summarizes the results of the optimization for both PWR and SPR sensors. In performing the comparison between the PWR and SPR sensors as depicted in Table 1 a few points are worth mentioning: 1) To model both sensors a transfer matrix method is used. 2) We have assumed that the substrate and prism are both BK7 glass. 3) Gold is used as the metallic layer, which is a preferred plasmonic layer. 4) Silica is used as the top dielectric layer in the PWR sensor which has a well-understood surface chemistry. 5) In the PWR sensor, the optimized values for the operating wavelength, silica thickness and gold thickness are 780nm, 545nm, and 48nm, respectively. 6) In the case of SPR sensor, the optimized values for the operating wavelength and gold thickness are 880nm and 50nm, respectively.

Table 1. Comparison of the optimized PWR and SPR sensors' characteristics

Sensor	polarization	$SF_{surf}$ (deg./nm)	$SF_{bulk}$ (deg./RIU)	SM (deg. <sup>-1</sup> )	$CSF_{surf}$ (nm <sup>-1</sup> )	$CSF_{bulk}$ (RIU <sup>-1</sup> )
PWR	1. TM	0.01	124	4.3	0.08	537
	TE	0.04	35	2.6	0.1	91
SPR	TM	0.1	176	0.57	0.06	101

## 4. Experimental setup

### 4.1 Sensors fabrication and functionalization

The BK7 glass slides coated with  $48 \pm 1$ nm gold layers, having an area of approximately 1cm  $\times$  1cm, were purchased from the SSENS Ltd [9]. To remove any organic contaminations the samples were initially cleaned with a piranha solution at 90°C for 20min and further cleaned in an ultrasonic bath with acetone, isopropanol, and deionized water for 10 minutes each. To fabricate our PWR sensors, a silica layer of 545nm thickness was deposited on the gold film using a plasma enhanced chemical vapor deposition (PECVD).

### 4.2 Instrumentation

Figure 2(a) illustrates the optical setup used to characterize the performances of the PWR and SPR sensors. A combination of a super continuum laser (Fianium SC-450), a laser line tunable filter (Photon Etc), and a single mode optical fiber is used for illumination. An achromatic lens (L1) is used to generate a collimated light which is then passed through a system composed of linear polarizer (P) oriented at 0 degrees and liquid crystal (LC) variable retarder (45 degrees orientations) acting as a polarization switch. In order to cover a desired range of angles, a second achromatic lens (L2) is used to achieve a converging beam. The converging beam is then focused onto the PWR or the SPR sensors through a prism and the reflected light is collected by a CMOS camera (Thorlabs). A Labview program was written to determine the minimum position of the angular curves by using a polynomial interpolation

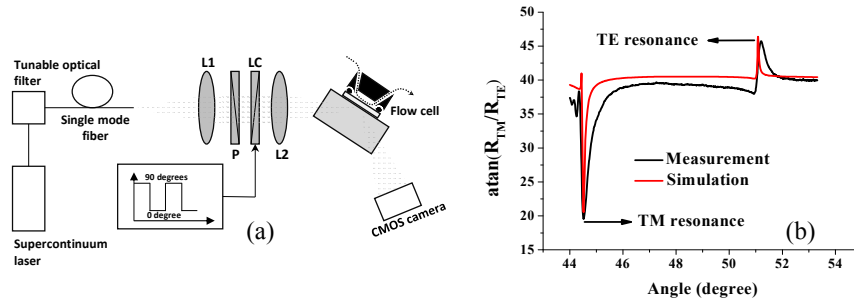


Fig. 2. (a) Optical setup used to detect the resonance angle. (b) The experimental (black line) and theoretical (red line) normalized reflectance spectrum of the PWR sensor.

Figure 2(b) shows the measured and calculated normalized reflectance spectrum. The black curve in Fig. 2(b) is the measured spectrum which has a dip close to  $44^\circ$  due to the TM mode resonance. There is also a second resonance at approximately  $51^\circ$  angle which corresponds to the TE mode. Note that since the TE reflectance is located in the denominator of the normalized spectrum it appears as a peak. The red curve in Fig. 2(b) is the reflectance spectrum calculated using the transfer matrix method. The simulated result is in agreement with the experiment in terms of the location of the resonance modes and the normalized reflectance values.

## 5. Self-referenced experiments

To investigate the response of the sensor to thin film adsorption, we used the biotin-streptavidin complex as it provides strong affinity and high specificity of interaction. To functionalize the SPR sensor with biotin, a solution of biotinylated PEG alkane thiol is passed over the SPR chip for two hours. On the other hand, the silica surface of the PWR sensor is functionalized with biotin by MicroSurfaces Inc [10]. The functionalized sensors are then fixed between the prism and the flow cell [Fig. 2(a)] using index matching oil. Figure 3 shows the measured sensograms of the SPR (only TM mode) and PWR (both TM and TE modes) to surface and bulk effects.

For all the surface adhesion measurements, phosphate buffered saline (PBS) solution is used as the buffer for the streptavidin diluted solution. The solutions were introduced to the sensor in the following order: (1) A pure PBS solution is passed over the sample for 25 minutes to create a baseline. (2) Then a  $1\mu\text{g/ml}$  streptavidin solution is passed through the flow cell for 25 minutes to study the sensor response to a low concentration of the Streptavidin. (3) A pure PBS solution is again passed to dissociate the weakly bounded molecules from the surface. (4) A  $10\mu\text{g/ml}$  streptavidin solution is passed for another 25 minutes to create a streptavidin saturated surface, and (5) another rinsing step is performed. (6) To investigate pure bulk refractive index variations on the sensors responses, PBS buffer solution is switched to deionized water (MilliQ  $18.2\text{ M}\Omega\cdot\text{cm}$ ). (7) A low concentration of salted water ( $0.01\text{M}$ ) is passed for 5 minutes followed by (8) deionized water. (9) A 1% Vol. ethanol solution (water diluted) was passed for another 5 minutes, and (10) deionized water flows over the sample to recreate the baseline.

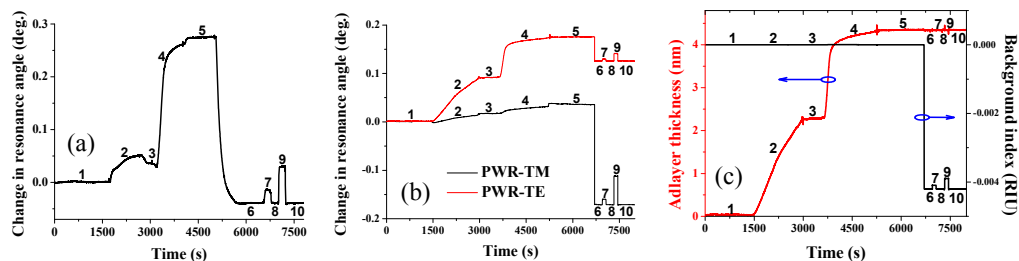


Fig. 3. (a) Angular positions of the resonance dip vs. time for the SPR sensor. (b) Angular positions of the resonance dip vs. time for the PWR sensor, TM and TE modes. (c) Surface binding thickness and bulk refractive index change calculated from (b). Solutions are (1) PBS, (2)  $1\mu\text{g/ml}$  Streptavidin, (3) PBS, (4)  $10\mu\text{g/ml}$  Streptavidin, (5) PBS, (6) DI water, (7)  $0.01\text{M}$  salted water, (8) DI water, (9) 1% ethanol, and (10) DI water.

Figure 3(a) shows the response of the SPR sensor, for the TM polarized light, to surface and bulk effects. Figure 3(b) is the response of the TE (red curve) and TM (black curve) modes of the PWR sensor to surface and bulk variations. Both curves have been measured simultaneously by tracing the resonance angles for each mode. As it can be seen from Fig. 3(b), the TE resonance angle experiences a larger change with respect to the surface variations as compared to the TM mode (steps 1 to 5), while the TM resonance angle is more affected by the change in the bulk refractive index (steps 6 to 10). Figure 3(c) shows the calculated

adlayer thickness change and bulk index variations as a function of time using the linear model given by Eqs. (3) and (4). The black line shows the background index change as a function of time and as it can be seen this response is almost constant during the streptavidin attachment (steps 1 to 5) and only changes when the variations in buffer refractive index are introduced (steps 6 to 10). The red line corresponds to the change in adlayer thickness which increases with the attachment of the streptavidin to biotin (steps 1 to 5) and remains constant when only the buffer refractive index changes (step 6 to 10). Therefore, the change in adlayer thickness is *completely decoupled* from the variations in bulk refractive index by using simultaneous dual polarization spectroscopy at a single sensing channel.

Table 2 summarizes the measured and calculated values of the SPR and PWR sensors' properties. The bulk sensitivity factor ( $SF_{bulk}$ ) for each sensor was measured by finding the change in resonance angle from the sensogram and the change in the refractive index of the buffer solution. This information along with the measured standard deviation of the sensors' outputs was used to calculate the bulk sensor *Resolution* [11] – i.e. the smallest detectable refractive index change per RIU – and is given in Table 2.

However, in the case of surface sensitivity factor ( $SF_{surf}$ ) it is more difficult to determine the exact thickness of the streptavidin layer experimentally; although it can be estimated from the simulation and assuming a refractive index of 1.5 for streptavidin at saturation [12]. We have estimated the thickness of the streptavidin to be 4.3nm which is close to its molecular size ( $4.5 \times 4.5 \times 5.8\text{nm}^3$ ) [13]; and the approximate values of the surface sensitivity ( $SF_{surf}$ ) are then calculated. Using the measured standard deviation of the sensors' outputs and the surface sensitivity factor, the values of LoD – defined as the smallest detectable concentration of analyte (ng/ml) – can be calculated and is given in Table 2.

From Table 2 it is clear that the LoD for the TE mode of the PWR is smaller than that of the TM mode of the PWR and the TM mode of the SPR. This makes the TE mode of the PWR an excellent choice for sensing surface effects, as it was discussed earlier. Similarly, the resolution of the TM mode of the PWR is smaller than that of the TE mode of PWR and TM mode of the SPR. This makes the TM mode of the PWR an excellent choice for sensing bulk effects, as discussed earlier. In addition, the simultaneous presence of TM and TE modes in the PWR allows us to adequately decouple the surface and bulk properties.

**Table 2. Experimental sensor' characteristics calculated from the sensograms shown in Fig. 3.**

Sensor	polarization	$SF_{surf}$ (deg./nm)	$SF_{bulk}$ (deg./RIU)	LoD (ng/ml)	Resolution (RIU)
PWR	TM	0.008	112	55	$2.6 \times 10^{-6}$
	TE	0.04	37	9	$7.4 \times 10^{-6}$
SPR	TM	0.06	154	63	$5 \times 10^{-6}$

## 6. Conclusion

In this paper a new approach for self-referenced biosensing was proposed and demonstrated based on a PWR sensor. The unique property of the PWR sensor, which is its polarization diversity, was utilized for dual-polarization spectroscopy. The TM mode of the PWR sensor demonstrated high sensitivity to the refractive index change in bulk solution while the TE mode was more sensitive to the thickness change of the attached streptavidin layer. The measured LoD for both TM and TE polarizations are 55 ng/ml and 9 ng/ml, respectively; and the measured resolution are  $2.6 \times 10^{-6}$  RIU and  $7.4 \times 10^{-6}$  RIU, respectively. Moreover, a linear model was used to decouple the change in adlayer thickness and the bulk refractive index from the sensor's response. Finally, the performance of the PWR sensor was compared to a SPR sensor, fabricated and tested under the same conditions. It was seen that the PWR sensor provides better LoD and resolution in addition to the ability to decouple surface and bulk effects.

## **Acknowledgments**

This work was supported by the Natural Science and Engineering Research Council of Canada–Biopsys Network under grant no. 486537.